Source Localization in Shallow Water Using a Neural Network Based on Range-Dependent Sound Speed Profile Model

Jing Guo[1, 2], Juan Zeng[1], Li Ma[1]

[1] *Key Laboratory of Underwater Acoustic Environment, Institute of Acoustics, Chinese Academy of Sciences, Beijing 100190, China*

[2] *University of Chinese Academy of Sciences, Beijing 100049, China*

Abstract **—** In range-dependent shallow-water environments, the complex spatiotemporal variations of the environmental sound speed profile (SSP) lead to mismatches between the SSP model and the actual environment, posing challenges in passive source localization. Leveraging the nonlinear feature extraction and pattern recognition capabilities of deep learning (DL) approaches, this paper investigates the range-dependent SSP model-based neural network for source localization. The performance of the network trained on a linear equivalent SSP model is evaluated, where the environmental SSP is parameterized as a linear function of range. The test results indicate that the neural network, after training on the dataset generated from the equivalent SSP model, demonstrates the ability to localize sources in range-dependent shallow-water environments. By applying transfer learning with experimental data from the Yellow Sea, the range-dependent network better fits the environmental model, leading to reduced errors and improved localization accuracy.

Key Words **—** source localization, deep learning, sound speed profile, range dependence, shallow water

1 Introduction

Passive source localization remains a critical topic in underwater acoustics. Numerous advanced methods based on matched-field processing (MFP) [1], such as matched-mode processing (MMP) [2] and matched-beam processing (MBP) [3], have been extensively developed. However, these methods are constrained in complex environments due to their dependence on the precise representation of environmental model. Especially shallow-water regions, where internal waves frequently induce strong spatiotemporal variability in the sound speed profile (SSP), present significant challenges. Such variability often leads to substantial mismatch between assumed algorithmic models and the actual environment conditions, resulting in notable performance degradation in MFP localization methods [4]~[7]. To address environmental uncertainties, Collins *et al.* [8],[9] introduced the focalization method, which jointly estimates both environmental parameters and source location by incorporating SSP model parameters into the optimization process. Nevertheless, conventional multi-parameter optimization algorithms, such as genetic algorithms (GA), suffer from slow convergence due to the high dimensionality and complexity of the parameter space. Additionally, the computational burden of generating replica fields constitutes an algorithmic constraint in practical MFP applications.

Recently, deep learning (DL) approaches [10] have emerged as promising tools for source localization, owing to their powerful nonlinear feature extraction and pattern recognition capabilities. In contrast to model-based MFP approaches, DL methods follow a data-driven paradigm, wherein neural networks autonomously learn latent features from acoustic data. Prior studies [11]~[13] have demonstrated the feasibility of using neural networks to directly map hydrophone signals to source locations, such as convolutional neural networks (CNNs) and long short-term memory (LSTM) networks. As DL approaches bypass the online acoustic field calculation, a properly offline trained neural network can reduce online computational costs relative to MFP approaches. Despite these advantages, DL localization approaches face two fundamental limitations:

(1) the lack of physical interpretability, with performance strongly reliant on data quality and quantity; and (2) the limited availability and high cost of acquiring real-world underwater acoustic data, which hampers the generation of high-quality training data and restricts network generalization and performance.

In this paper, a hybrid method is proposed that integrates MFP with DL approach for passive source localization in shallow-water environments. Specifically, training data are generated using a range-dependent equivalent SSP model that characterizes the primary variability of the environmental SSP, thereby enabling effective training of the neural network. The training set consists of all acoustic samples generated within a given parameter space and can be regarded as a set of precomputed replica fields based on the equivalent SSP model. A linear equivalent SSP model that characterizes the range dependence of the environmental SSP influenced by internal waves is employed. The neural network is able to learn from the precomputed replica samples of the training set and utilize the learned features to identify the inputs from unknown environments. This process is functionally equivalent to matching measured samples with precomputed replica samples through a neural network, while preserving partial physical relevance through model-based feature construction. The pretrained network demonstrates effective source localization performance on the validation set, confirming the feasibility of the proposed method. Following pretraining, transfer learning (TL) [15] ~ [19] is employed to further improve the network's localization accuracy and generalization in real-world conditions. A limited number of measured acoustic samples are used to fine-tune the pretrained network, enabling better adaptation to actual environmental. The transfer-learned network performs well on the experimental test set, further validating the effectiveness of the proposed hybrid method based on the range-dependent equivalent SSP model.

2 Localization algorithms

2.1 Range-dependent equivalent SSP model

In conventional MFP localization methods, empirical orthogonal functions (EOFs) are commonly used as basis functions to construct a range-independent equivalent SSP, which serves to mitigate model mismatch caused by temporal variations in the SSP [8][20]. The range-independent equivalent SSP model can be expressed as

$$C(z) \simeq C_0(z) + \sum_{m=1}^{M} \varphi_C^m A_m \,. \tag{1}$$

Here φ_C^m and A_m denote the m^{th} basis function and its corresponding coefficient, respectively. The background SSP (C_0) is typically obtained by averaging historical SSP measurements and the basis functions (*e.g.*, EOFs) are also extracted from historical data, thereby leveraging environmental prior information [20]. This range-independent equivalent SSP model effectively captures the vertical structure of the environmental SSP. When the range dependence of the environmental SSP is weak, the model yields satisfactory localization performance. However, its inability to account for range-dependent variations limits its applicability in shallow-water environments influenced by internal waves.

By incorporating the range-dependent variation into the previously mentioned range-independent equivalent SSP model, the resulting model acquires the ability to capture the range dependence of the environmental SSP. Within short range intervals, the environmental SSP is assumed to vary slowly and can be approximated as a linear function of range [14]. Dividing the environmental SSP into L range segments, and the range-dependent SSP is then approximated by linear profiles over these segments. The linear equivalent SSP model can be expressed as

$$\widehat{\boldsymbol{C}} \simeq \left\{ \left[\hat{C}_1 \sim \hat{C}_2\right]_1, \cdots, \left[\hat{C}_l \sim \hat{C}_{l+1}\right]_l, \cdots, \left[\hat{C}_L \sim \hat{C}_{L+1}\right]_L \right\}, \tag{2}$$

$$\hat{C}_l(z) \simeq C_0(z) + \sum_{m=1}^{M} \varphi_m^l A_m^l \,, \tag{3}$$

where $\left[\hat{C}_l \sim \hat{C}_{l+1}\right]_l$ denotes that the SSP within the l^{th} segment varies linearly from $\hat{C}_l$ to $\hat{C}_{l+1}$ over range. Under the linear equivalence condition, the linear equivalent SSP model can represent the primary spatial variations of the environmental SSP.

However, the selection of segment intervals largely depends on empirical experience and environmental prior information.

In shallow-water environments, internal wave activity is typically dominated by a primary tidal constituent, inducing pronounced sound speed fluctuations that exhibit strong tidal periodicity. In shallow regions of the Yellow Sea, where internal waves are prominent, the semi-diurnal tidal constituent (M2) dominates the dynamics [21]. Under such conditions, the vertical structure of environmental SSP, such as the thermocline, can be effectively parametrized by a background SSP C_0 and basis function φ_C, both derived from 12-hour SSP measurements covering a full semi-diurnal tidal cycle. Given the background SSP and the basis functions, the linear equivalent SSP model can then be parameterized by a coefficient matrix β corresponding to the basis functions.

$$\beta = \begin{bmatrix} A_{1,1} & \cdots & A_{1,M} \\ \vdots & \ddots & \vdots \\ A_{L+1,1} & \cdots & A_{L+1,M} \end{bmatrix}. \tag{4}$$

The coefficient matrix β contains a total of $(L+1) \times M$elements, where L denotes the number of linear segments used to model the range dependence of the SSP, and M represents the number of basis functions. By incorporating the linear equivalent SSP model to MFP framework, the broadband source localization problem is reformulated to a nonlinear multi-parameter optimization problem with the Bartlett processor [1][4]

$$(\alpha, \beta, r, z) = max\{F(\alpha, \beta, r, z)\}, \tag{5}$$

$$F(\alpha, \beta, r, z) = \frac{1}{N_f}\sum_{j=1}^{N_f} |\boldsymbol{V}_{\alpha,\beta,r,z}^{H}\boldsymbol{X}|^2. \tag{6}$$

Here r denotes source range,z denotes source depth, and α represents additional unknown environmental parameters. N_f is the number of frequency points used in MFP. The objective of the optimization is to maximize the correlation between the measured field vector $\boldsymbol{X}$, and the replica field vector $\boldsymbol{V}_{\alpha,\beta,r,z}$.

Numerical simulation is performed using the MFP algorithm based on a linear equivalent SSP model to assess its performance. The simulation environment is constructed using SSP measurements collected during the 2011 Yellow Sea experiment, as illustrated in Fig. 1(a), with a constant water depth of 40 m and a semi-infinite bottom. The linear equivalent SSP model is divided into three segments ($L = 3$), each spanning

a range interval of 4000 m in the simulation. Only the first EOF ($M = 1$), derived from the simulated environmental SSP, is used as the basis function. Environmental parameters, including seabed properties, the vertical line array (VLA) configuration, and the source location, are summarized in Table 1. The acoustic field is computed using the range-dependent acoustic model (RAM) with a maximum range of 12 km and a range step of 10 m. The genetic algorithm (GA) used in the MFP optimization adopts a generation gap of 0.9, a crossover probability of 0.9, a mutation probability of 0.05, and parallel processing with 40 individuals over 50 generations, resulting in 2000 parameter evaluations. Table 2 presents the parameter search ranges and the localization results obtained by the MFP algorithm based on the linear equivalent SSP model.

Tab. 1. Simulation environment parameter settings.

Seabed			Vertical line array			Source		
sound speed	density	attenuation	element count	element spacing	depth coverage	range	depth	signal frequency
m/s	g/cm^3	dB/λ	\	m	m	km	m	Hz
1600	1.5	0.25	16	1.5	12.5~35	10	25	650 700 750 800 850

Tab. 2. Parameter search ranges and MFP result in simulation.

	Equivalent SSP model				Source	
Parameter search ranges	A_1	A_2	A_3	A_4	range (km)	depth (m)
	[-20,30]	[-20,30]	[-20,30]	[-20,30]	[8,12]	[5,40]
MFP result	-0.27	22.27	-19.32	2.32	9.9	25

For shallow-water source localization, numerical simulation demonstrates that the linear equivalent SSP model effectively captures primary features of range-dependent environmental SSP and enables accurate source localization. Figure 1(b) shows the reconstructed equivalent SSP, while Fig. 1(c) presents the estimated localization ambiguity surface. It can be observed that the equivalent SSP model adapts to range-dependent environmental variations by adjusting the model parameters $A_1 \sim A_4$, and the optimal parameters are obtained during the optimization process, yielding an accurate

source location estimate (9.9 km / 25 m). The simulation results indicate that the linear equivalent SSP model successfully characterizes the range-dependence of the environmental SSP and can be effectively integrated into localization algorithms under shallow-water internal wave conditions. More detailed studies of the range-dependent MFP methods will be presented in other separate works by the authors.

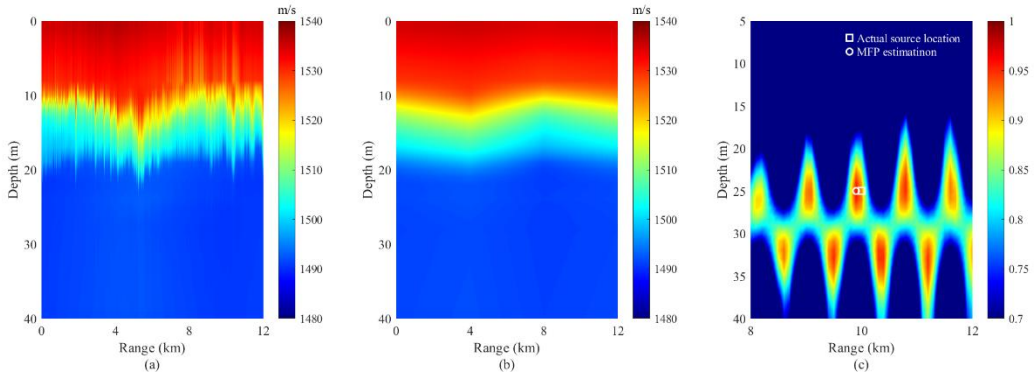

Fig.1 Range-dependent MFP localization.

(a) Simulated environmental SSP; (b) Reconstructed equivalent SSP;

(c) Localization ambiguity surface.

2.2 Model-based deep learning

By rewriting Eq. (6) in vector form, the MDP can be interpreted as a weighted correlation measure. Specifically, the replica vector $\boldsymbol{P}_r$, received by an array with N elements located at depths z_N, is transformed into a covariance matrix $\boldsymbol{R}_{Pr}$, which is then used to perform a weighted correlation with the measured vector $\boldsymbol{P}$, where (r, z) denotes the actual source location. The localization ambiguity function $A(\boldsymbol{P}, \boldsymbol{P}_r)$ is evaluated over a search grid to form the ambiguity surface:

$$A(\boldsymbol{P}, \boldsymbol{P}_r) = \frac{\boldsymbol{P}\boldsymbol{R}_{Pr}\boldsymbol{P}^*}{\|\boldsymbol{P}\|_2^2 \|\boldsymbol{P}_r\|_2^2}, \tag{7}$$

$$\boldsymbol{R}_{Pr} = \boldsymbol{P}_r^* \boldsymbol{P}_r, \tag{8}$$

$$\boldsymbol{P} = [P(r, \mathrm{z}, z_1) \quad \cdots \quad P(\mathrm{r}, \mathrm{z}, z_N)], \tag{9}$$

$$\boldsymbol{P}_r = [P_r(r', z', z_1) \quad \cdots \quad P_r(r', z', z_N)]. \tag{10}$$

Each point on the localization ambiguity surface corresponds to a candidate source location (r', z') in the replica model, along with the replica covariance matrix $\boldsymbol{R}_{Pr}$. However, the optimal model parameters are obtained through the iteratively and

randomly searching within the parameter space. Due to the need to traverse nearly the entire parameter space, conventional nonlinear multi-parameter optimization algorithm (*e.g.*, the genetic algorithm) suffers from high computational cost and require repeated searching for each localization task, which results in substantial online computational burden. From an algorithmic perspective, offline precomputation of extensive replica samples ($\boldsymbol{R}_{Pr}$) allows the online stage to bypass parameter searching and directly identify the measured samples against the precomputed database, resulting in substantial reductions in computational load and processing time. Data-driven DL approaches exhibit potential for this identification task, leveraging their inherent capabilities in nonlinear feature extraction and pattern recognition. Notably, prior study has shown that neural networks can effectively emulate MFP [22][23].

This section discusses a range-dependent neural network for source localization in shallow-water environments influenced by internal waves, integrating MFP with DL approaches. A range-dependent equivalent SSP model—such as the linear equivalent SSP model mentioned in Sec. 2.1—is employed to generate training data. This approach is equivalent to precomputing a large set of replica samples offline and replacing conventional parameter optimization and matching processes with a neural network. By training the network with model-generated data, the reliance on extensive real-world acoustic data is reduced. The range-dependent network extracts generalizable features from the replica samples for source localization, and higher localization accuracy can be further achieved through transfer learning using limited amount of real-world measured data. The network is adapted from the multi-task learning U-Net described in Ref. [23], with the preprocessing procedure and overall network architecture briefly illustrated in Figs. 2 and 3. The source localization algorithm based on the range-dependent neural network is implemented as follows:

(1) Using the linear equivalent SSP model, which has been validated for source localization in range-dependent environment, numerous SSPs are generated over a given model parameter grid. Based on these SSPs, the corresponding replica acoustic fields are computed as replica samples, which are then converted into feature maps through a preprocessing procedure to form the training set. Details of the training,

validation, and test sets are provided in Sec. 2.3.

(2) After pretraining, the neural network approximates the source localization system based on the linear equivalent SSP model. The performance of the pretrained network on the validation set is presented in Sec. 3.1. A limited amount of experimental data is used to fine-tune the pretrained network via transfer learning, completing the full source localization workflow. The performance of both the pretrained and transfer-learned networks on the experimental test set is discussed in Sec. 3.2.

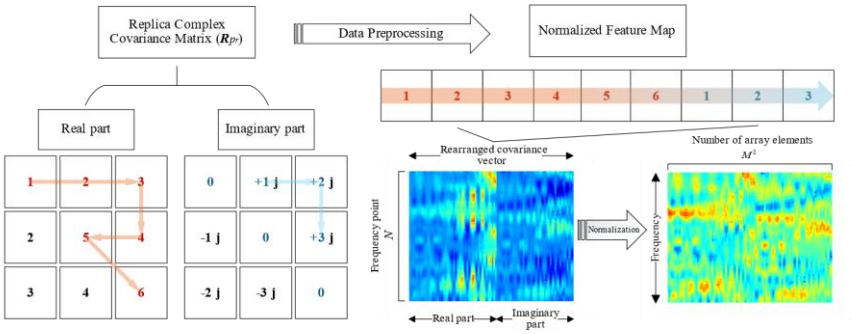

Fig.2 Data preprocessing of the replica samples.

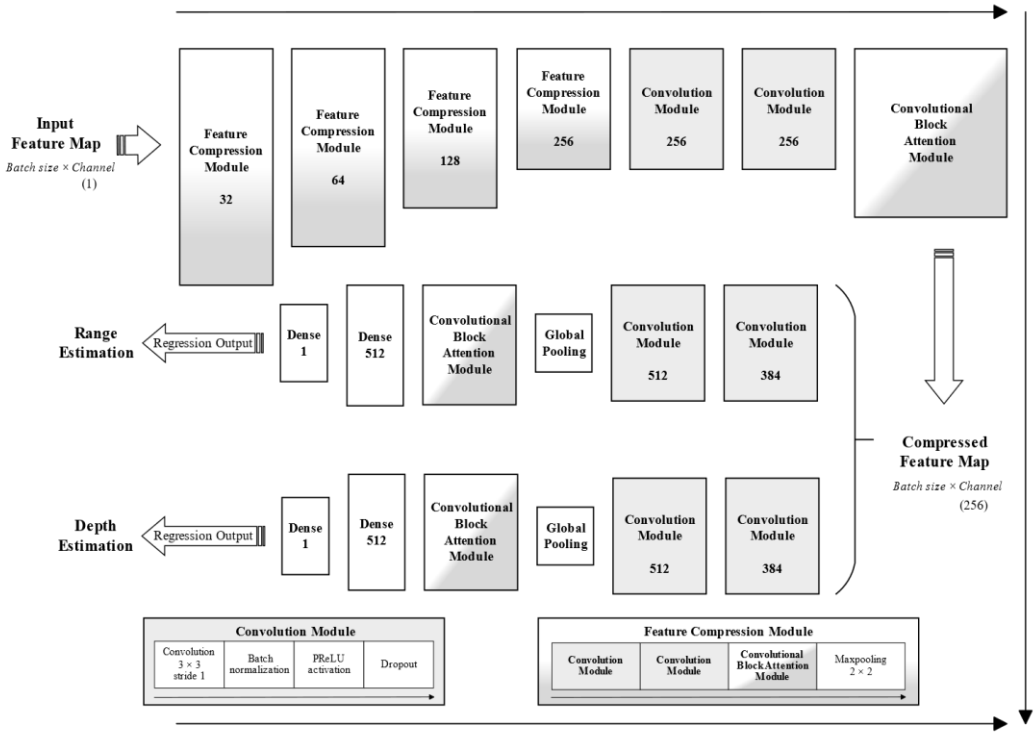

Fig.3 Multi-task learning U-Net framework for source localization.

2.3 Datasets generation

In the summer of 2011, the Institute of Acoustics, Chinese Academy of Sciences, conducted an underwater acoustic propagation experiment in the shallow region of the Yellow Sea, where significant internal wave activity was present. The experimental deployment is shown in Fig. 4. The water depth is 40 m, with the source located at a depth of 22 m and a range of 10 km from the receiving VLA. The source emitted linear frequency modulated (LFM) signals ranging from 650 to 850 Hz, with a modulation duration of 3 s and a repetition interval of 45 s. The receiving VLA consisted of 16 hydrophones, with the uppermost hydrophone positioned at 12.5 m depth and the lowermost at 35 m, spaced at 1.5 m intervals. A temperature-depth (TD) sensor array near the receiving VLA recorded internal wave activity dominated by the semidiurnal tide. Figure 5(b) shows the 36-hour SSP measurements in the experiment. The first three EOFs [Fig. 5(a)] extracted from the 12-hour SSP measurements indicated in Fig. 5(b)—corresponding to the semidiurnal tidal period—serve as the basis functions for the linear SSP model.

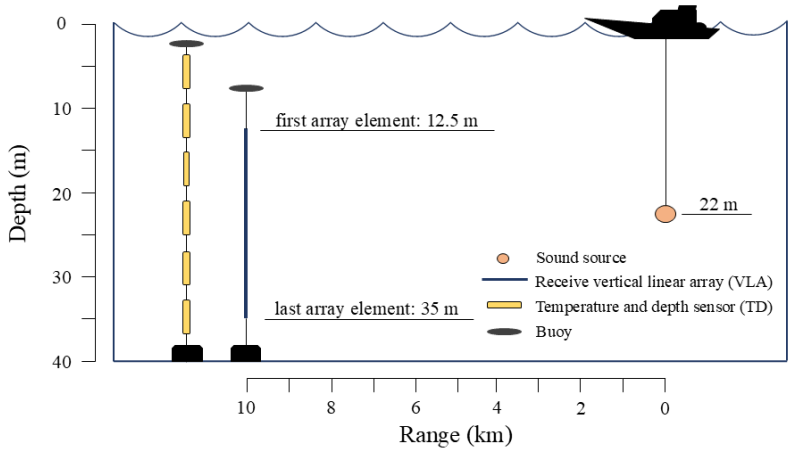

Fig.4 The deployment of the 2011 summer experiment in the Yellow Sea.

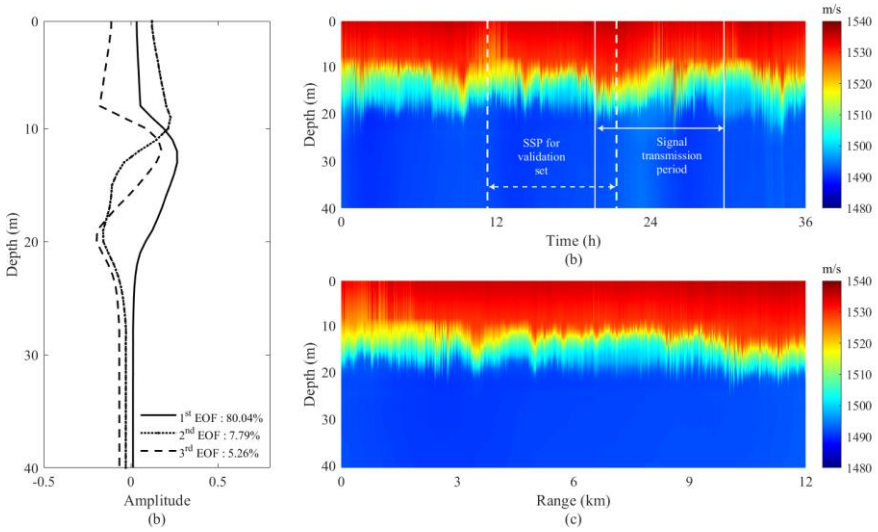

Fig. 5 Information of environmental SSP characteristics.

(a) The first three EOFs; (b) 36-hour real-world SSP measurements;

(c) 12-km range-dependent SSP for validation set generation.

Environment-representative linear equivalent SSPs are constructed to generate the training set, while the maximum computation range for acoustic field is set to 12 km. When the first-order EOF is used as the basis function ($M = 1$), the linear equivalent SSP model requires only the given model parameters

$$Paralist = \begin{bmatrix} \boldsymbol{\beta}_1 \\ \vdots \\ \boldsymbol{\beta}_N \end{bmatrix} = \begin{bmatrix} A_1^1 & \cdots & A_{L+1}^1 \\ \vdots & \ddots & \vdots \\ A_1^N & \cdots & A_{L+1}^N \end{bmatrix}. \tag{6}$$

Consistent with the MFP simulation in Section 2.1, set $L = 3$ (range interval of 4000 m) to construct equivalent SSPs. Here, N represents the total number of equivalent SSPs to be constructed. The EOF coefficient A varies from -20 to 30 in increments of 10, producing a total of $N = 1296$ SSPs. Table 3 summarizes the environmental parameter settings used for replica samples generation. The complete training set consists of 265,680 replica samples, generated from all combinations of: 1296 SSPs, 41 source ranges, 5 source depths, and 3 sea depths. Meanwhile, the validation set for evaluating the range-dependent network's localization performance is generated using the 12-km SSP shown in Fig. 5(c). This range-dependent SSP is derived from SSP measurements and extended according to an internal wave propagation speed of 0.33 m/s [21]. As specified in Table 3, the validation set comprises 123 simulated samples (41

source ranges × 3 source depths).

Tab. 3 Configuration of grid parameters for datasets generation

	Sea depth m	Source range km	Range interval km	Source depth m	Depth interval m	Signal frequency Hz	Frequency interval Hz
Training Set	38 40 42	8 ~ 12	0.1	10 ~ 30	5	650 ~ 850	1
Validation Set	40	8 ~ 12	0.1	10 ~ 30	10	650 ~ 850	1

3 Simulation and experimental data evaluation

3.1 Validation set performance

The training set incorporates extensive synthetical range-dependent features of the linear equivalent SSP model, while the neural network learns these characteristics through feature extraction to enhance source localization performance. During network training, the learning rate is set to 10^{-3} and batch size to 4 for 5 epochs. Other network parameters not explicitly mentioned are set according to Ref. [23]. The training is conducted on a platform equipped with an *Intel(R) Core(TM) Ultra 5 125H* CPU and an *Nvidia GeForce RTX 4060 Laptop GPU*, with a total training time of approximately 12 hours. The training loss curve and mean absolute errors (MAEs) for range and depth estimation are shown in Fig. 6. Both the loss curve and MAE trends indicate that the network effectively converges.

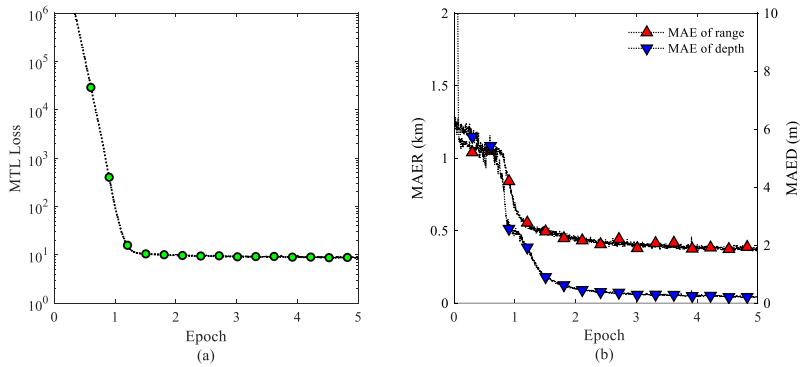

Fig. 6 Training process of range-dependent network.

(a) MTL loss curve; (b) MAEs of range and depth estimation.

The validation set consists of replica samples with a fixed sea depth of 40 m and source depths of 10 m, 20 m, and 30 m. Figure 7(a) presents the source ranges estimated by the range-dependent network on the validation set, while Fig. 7(b) shows the MAEs of range and depth estimates under the three source depth conditions. The network successfully captures variations in source range, indicating effective learning of range-dependent features from the extensive replica samples generated by the linear SSP model. Consequently, the estimated source range curves on the validation set closely follow the trend of the actual range variation. The network yields relatively accurate estimates for sources at 20 m depth. While discrepancies between the linear equivalent SSP model and the environmental SSP model result in localization errors (MAE < 1.5 km in range and MAE < 7 m in depth), the errors remain within acceptable bounds. These results support the feasibility of replacing conventional parameter optimization (e.g., genetic algorithm) in MFP localization algorithm with DL approach. In particular, the neural network is capable of learning key features from the linear equivalent SSP model, achieving practically acceptable localization performance in range-dependent shallow-water environments.

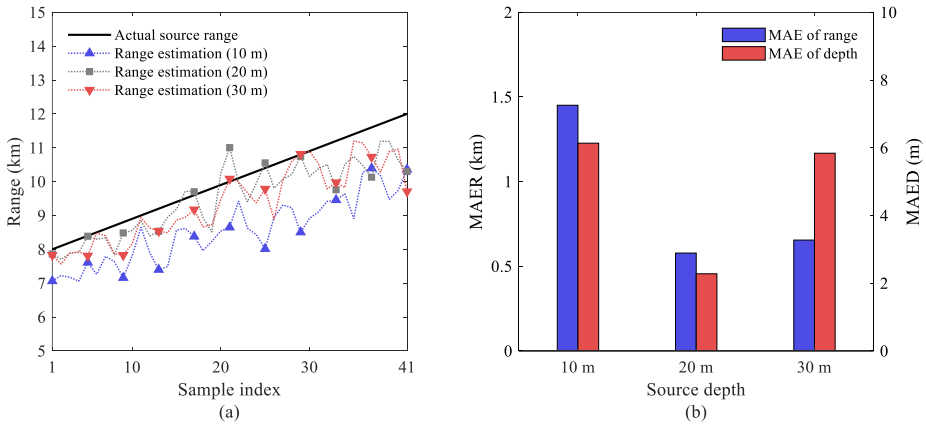

Fig. 7 Network performance on the validation set.

(a) Estimation curves of source location; (b) MAEs of source localization.

3.2 Transfer learning and generalization testing

Although the pretrained network exhibits preliminary localization capability, its performance in complex real-world environments requires further enhancement via

transfer learning. The feature compression module remains frozen to preserve learned representations, while the downstream output layers are fine-tuned using experimental data. This strategy theoretically maintains the network's performance in the source domain (the equivalent SSP model) while improving its generalization ability in the target domain (environmental SSP model). The experimental test set includes 300 received signals from the 2011 Yellow Sea experiment, with a signal-to-noise ratio (SNR) of approximately 16 dB estimated via spectral analysis. Another 200 received signals from the experiment are used as the transfer set. For the transfer learning, learning rate of 10^{-4} with batch size 1 across 10 epochs are employed. The pretrained and transfer-learned networks are evaluated on the experimental test set. Due to the unaffordable computational demands of the linear model-based MFP method (about 300-hours processing time with convergence-ensuring iterations in the real-world environment), the range-independent normal MFP is employed for comparison. The normal MFP utilizes a single experimental SSP measured at the receiving VLA.

Figure 8 shows the estimated results of the pretrained network, the transfer-learned network, and the normal MFP method on the experimental test set, while Fig. 9 presents the corresponding MAEs of source localization. The pretrained network's range estimation curve confirms preliminary source localization capability in experimental range-dependent environment. After pretraining, the range-dependent network significantly outperforms the normal MFP method on the experimental test set, with a range estimation MAE of 0.91 km, much smaller than the 2.93 km MAE of the normal MFP. However, the pretrained network's depth estimation performance is comparable to that of the normal MFP method, with depth estimation MAEs of 10.8 m and 11.8 m, respectively. This implies that range-dependence of the SSP may not be the decisive factor for source depth estimation. Depth estimation accuracy remain constrained by other parameter mismatches, including receiving array configuration, SSP vertical structure, and source depth itself (as indicated by the different MAE levels at different source depths shown in Fig. 7), along with other possible factors. By further learning from experimental data, the transfer-learned network yields substantial improvement in depth estimation and modest range accuracy enhancement. The depth estimation MAE

of the transfer-learned network is reduced to 4.1 m, which is less than half that of the pretrained network. The range estimation MAE of the transfer-learned network decreases to 0.84 km. The enhancement can be reasonably attributed to the transfer set providing the network with supplementary real-world environmental information, thereby significantly improving both depth estimation accuracy and the generalization capability of the range-dependent network.

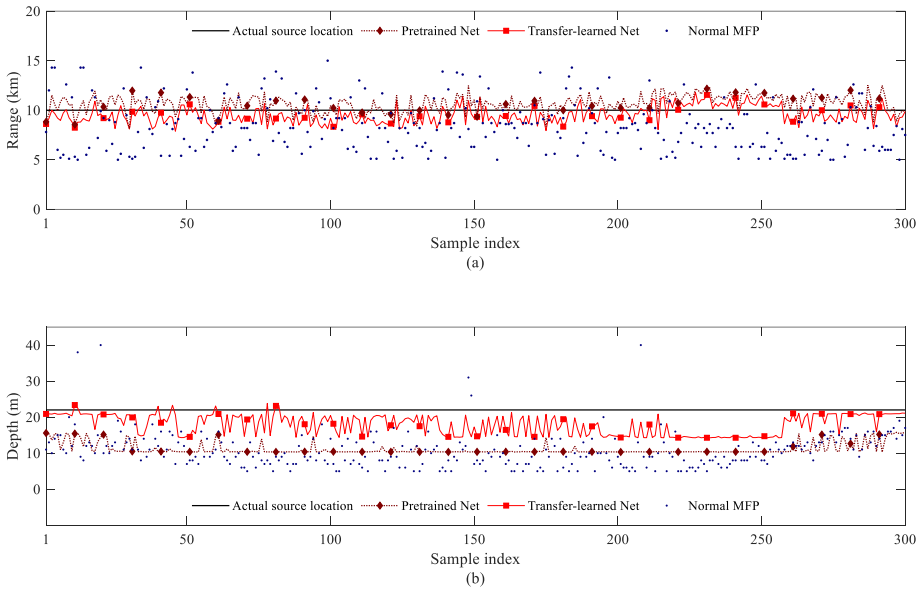

Fig. 8 Algorithms performance on the experimental test set.

(a) Estimation of source range; (b) Estimation of source depth.

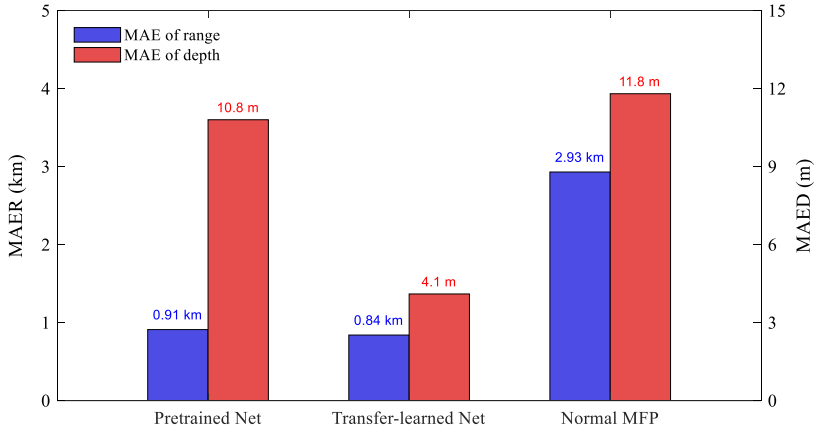

Fig. 9 MAEs of source localization algorithms.

4 Conclusion

For the shallow-water internal wave environment in the Yellow Sea, this study employs a linear equivalent SSP model to generate replica samples. The extensive replica samples are subsequently utilized to train the neural network for source localization in range-dependent environments. Transfer learning based on limited experimental data further improves the network's adaptation to the environmental model and enhances its generalization capability. From the MFP perspective, this hybrid method effectively replaces conventional parameter optimization algorithms (*e.g.*, genetic algorithms) in MFP methods with neural networks. The offline trained network utilizes learned replica samples to identify and estimate unknown measured inputs, thereby reducing the online computational burden of MFP methods. Taking the platform and experimental test set in this study as an example, linear model-based MFP method would require approximately 300 hours of online computation to completes estimation of the test set. In contrast, after 12 hours of offline network training, the range-dependent neural network completes estimation of the test set in merely 40 seconds of online computation. From the DL perspective, the range-dependent equivalent SSP model constrains the feature distribution of the training set. The neural network extracts and learns sufficient synthetic sound speed variation patterns from the training set, effectively mitigating the shortage of measured data for DL methods. Specifically, the proposed range-dependent network is trained primarily on model-generated data, with transfer learning performed using only 200 experimental received signals.

The performance of the proposed hybrid method on both the validation set and experimental test set confirms its effectiveness for source localization in range-dependent shallow-water environments. Future researches on the range-dependent network may include: (1) development of improved range-dependent equivalent SSP models tailored to diverse acoustic environments, and (2) optimization of network architectures to enhance localization performance.

References

[1] Homer P. Bucker, “Use of calculated sound fields and matched-field detection to locate sound sources in shallow water,” *J. Acoust. Soc. Am.*, vol. 59, no. 2, pp. 368–373, 1976, doi: 10.1121/1.380872.

[2] Yoo K and Yang TC, “Broadband source localization in shallow-water in the presence of internal waves,” *J. Acoust. Soc. Am.*, vol. 106, pp. 3255–3269, 1999, doi: 10.1121/1.428179.

[3] Yang TC and Yates T, “Matched-beam processing: application to a horizontal line array in shallow-water,” *J. Acoust. Soc. Am.*, vol. 104, pp. 1316–1330, 1998, doi: 10.1121/ 1.424341.

[4] Rachel M. Hamson and Richard M. Heitmeyer, “Environmental and system effects on source localization in shallow water by the matched-field processing of a vertical array,” *J. Acoust. Soc. Am.*, vol. 86, pp. 1950-1959, 1989, doi: 10.1121/1.398573.

[5] Cristiano Soares, Martin Siderius, and Sergio M. Jesus, “Source localization in a time-varying ocean waveguide,” *J. Acoust. Soc. Am.*, vol. 112, pp. 1879-1889, 2002, doi: 10.1121/1.1508786.

[6] Peter Gerstoft and Donald F. Gingras, “Parameter estimation using multifrequency range-dependent acoustic data in shallow water,” *J. Acoust. Soc. Am.*, vol. 99, pp. 2839-2850, 1996, doi: 10.1121/1.414818.

[7] A.G. Sazontov and I.P. Smirnov, “Source Localization in an Acoustic Waveguide with Inaccurately Known Parameters Using Matched Processing in the Mode Space,” *Acoust. Phys*., vol. 65, pp. 450-459, 2019, doi: 10.1134/S1063771019040171.

[8] Michael D. Collins and W. A. Kuperman, “Focalization: Environmental focusing and source localization,” *J. Acoust. Soc. Am.*, vol. 90, pp. 1410-1422, 1991, doi: 10.1121/1.401933.

[9] Ralph N. Baer and Michael D. Collins, “Source localization in the presence of internal waves,” *J. Acoust. Soc. Am.*, vol. 118, pp. 3117-3121, 2005, doi: 10.1121/1.2041331.

[10] LeCun Y, Bengio Y and Hinton G, “Deep learning,” *Nature*, vol. 521, pp. 436–444, 2015, doi: 10.1038/nature14539.

[11] S. K. R. Prasad and S. Gurugopinath, “Deep Learning Techniques for Detection of Underwater Acoustic Sources,” *2023 11th International Conference on Internet of Everything, Microwave Engineering, Communication and Networks (IEMECON)*, Jaipur, India, pp. 1-6, 2023, doi: 10.1109/IEMECON56962.2023.10092324.

[12] Li X, Song W, Gao D, Gao W and Wang H, “Training a U-Net based on a random mode-coupling matrix model to recover acoustic interference striations,” *J. Acoust. Soc. Am.*, vol. 147, pp. EL363–369, 2020, doi: 10.1121/10.0001125.

[13] Liu Y, Niu H, and Li Z, “A multi-task learning convolutional neural network for source localization in deep ocean,” *J. Acoust. Soc. Am.*, vol. 148, pp. 873–883, 2020, doi: 10.1121/10.0001762.

[14] Harry A and DeFerrari, “Effects of horizontally varying internal wavefields on multipath interference for propagation through the deep sound channel,” *J. Acoust. Soc. Am.*, vol. 56, no. 1, pp. 40–46, 1974, doi: 10.1121/1.1903230.

[15] Niu H, Reeves E, and Gerstoft P, “Source localization in an ocean waveguide using supervised machine learning,” *J. Acoust. Soc. Am.*, vol. 142, pp.1176–1188, 2017, doi: 10.1121/1.5000165.

[16] Huang Z, Xu J, Gong Z, Wang H and Yan Y, “Source localization using deep neural networks in a shallow-water environment,” *J. Acoust. Soc. Am.*, vol. 143, pp. 2922–2932, 2018, doi: 10.1121/1.5036725.

[17] Yoon S, Yang H and Seong W, “Deep learning-based high-frequency source depth estimation using a single sensor,” *J. Acoust. Soc. Am.*, vol. 149, pp. 1454–1465, 2021, doi: 10.1121/10.0003603.

[18] Liu Y, Niu H, and Li Z, “Source ranging using ensemble convolutional networks in the direct zone of deep water,” *Chinese Phys. Lett.*, vol. 36, no. 4, pp. 044302, 2019, doi: 10.1088/ 0256-307X/36/4/044302.

[19] Wang W, Ni H, Su L, Hu T, Ren Q, Gerstoft P, et al, “Deep transfer learning for source ranging: deep-sea experiment results,” *J. Acoust. Soc. Am.*, vol. 146, pp. EL317–322, 2019, doi: 10.1121/1.5126923.

[20] Lester R. LeBlanc and Forster H. Middleton, “An underwater acoustic sound velocity data model,” *J. Acoust. Soc. Am.*, vol. 67, pp. 2055-2062, 1980, doi: 10.1121/1.384448.

[21] Tao Hu, Zhen Wang, S. M. Guo, Li Ma, “Inversion of the internal wave velocity using the normal-mode amplitude fluctuation of an underwater sound field,” *Journal of Harbin Engineering University*, vol. 41, no. 10, pp. 1518-1523, 2020, doi: 10.11990/jheu.202007063.

[22] M.D. Liu, H. Q. Niu, and Z. L. Li, “Implementation of Bartlett matched-field processing using interpretable complex convolutional neural network,” *JASA Express Lett.*, vol. 3, no. 2, pp. 026003, 2023, doi: 10.1121/10.0017320.

[23] Peng Qian, W. M. Gan, H. Q. Niu, G. h. Ji, Z. L. Li, and G. J. Li, “A feature-compressed multi-task learning U-Net for shallow-water source localization in the presence of internal waves,” *Applied Acoustics*, vol. 211, no. 109530, 2023, doi: 10.1016/j.apacoust.2023.109530.